

DISCOVERY OF A 75 DAY ORBIT IN XTE J1543–568

J. J. M. IN 'T ZAND¹

Astronomical Institute, Utrecht University, P.O. Box 80000, NL-3508 TA Utrecht, Netherlands; jeanz@sron.nl

AND

R. H. D. CORBET² AND F. E. MARSHALL

NASA Goddard Space Flight Center, Laboratory for High Energy Astrophysics, Code 662, Greenbelt, MD 20771;

corbet@lheamail.gsfc.nasa.gov, marshall@lheamail.gsfc.nasa.gov

Received 2001 March 8; accepted 2001 April 27; published 2001 May 22

ABSTRACT

Dedicated monitoring of the transient X-ray pulsar XTE J1543–568 during the first year after its discovery has revealed the unambiguous detection of a binary orbit. The orbital period is 75.56 ± 0.25 days, and the projected semimajor axis is 353 ± 8 lt-s. The mass function and position in the pulse period versus orbital period diagram are consistent with XTE J1543–568 being a Be X-ray binary. The eccentricity of less than 0.03 (2σ) is among the lowest for the 12 Be X-ray binaries whose orbits have now been measured. This confirms the suspicion that small kick velocities of neutron stars during supernovae are more common than expected. The distance is estimated to be larger than 10 kpc and the luminosity at least 10^{37} ergs s^{-1} .

Subject headings: binaries: general — pulsars: individual (XTE J1543–568) — X-rays: stars

1. INTRODUCTION

The transient X-ray source XTE J1543–568 was discovered during a slew of the Proportional Counter Array (PCA) on the *Rossi X-Ray Timing Explorer* (*RXTE*) on 2000 February 6.84, when it had a 2–10 keV flux of 2×10^{-10} ergs $cm^{-2} s^{-1}$ (Marshall, Takeshima, & In 't Zand 2000). A subsequent pointed PCA observation on February 10.69 showed a similar intensity and revealed a pulsar with a period of 27.12 ± 0.02 s. Later, the pulsar was found in earlier data from the Burst and Transient Source Experiment (BATSE) on the *Compton Gamma Ray Observatory*; the first detection of the pulsar was on January 25 (Finger & Wilson 2000). The most accurate location was recently determined by serendipitous observations with the Wide Field Cameras on *BeppoSAX*: $\alpha_{2000.0} = 15^h 44^m 01^s$, $\delta_{2000.0} = -56^\circ 45' 9''$ with a 99% confidence region delimited by a circle with a radius of 2'0 (Kaptein, in 't Zand, & Heise 2001). Thus far, no optical counterpart has been reported.

XTE J1543–568 continues to be active 1 yr after discovery and is being monitored through regular pointed PCA observations. We here discuss the results from a timing analysis of data from the first year of monitoring and report the discovery of the binary orbit of XTE J1543–568, present the light curve, and discuss implications for the companion of the neutron star.

2. OBSERVATIONS AND DATA ANALYSIS

A target-of-opportunity program was initiated after the discovery with *RXTE* to monitor the pulsar and to try to detect Doppler delays from a binary orbit. The frequency of the observations went from once every day for the first 7 days to once every 2 days during the next 10 days, to once every 3 days during the next 75 days, and finally to once every week for the remainder of the time. Weekly observations still continued 1 yr after discovery. We here report about the first year of observations (i.e., up to 2001 February 3), for which the total accumulated net exposure time is 172 ks. The number of observations is 77. Most observations were carried out over two consecutive

RXTE orbits with a total span of 1.9 hr, but the time span has been as high as 5.5 hr. We discuss measurements that were carried out with the PCA on *RXTE*. This instrument (for a detailed description, see Jahoda et al. 1996) consists of an array of five co-aligned proportional counter units (PCUs) that are sensitive to photons of energy 2–60 keV with a total collecting area of 6500 cm^2 . The spectral resolution is 18% FWHM at 6 keV, and the field of view is 1° FWHM. During the observations the number of active PCUs varied between 1 and 5.

2.1. Light Curve

We extracted spectra for each *RXTE* orbit of observation, for all active PCUs combined and for layer 1 only. All spectra were successfully modeled between 3 and 20 keV using a power-law function with low-energy absorption (following Morrison & McCammon 1983), multiplied by an exponential cutoff function and supplemented with a narrow emission line near 6.5 keV that may be identified with Fe K line emission for neutral to carbon-like ionization states and which has a constant equivalent width of 127 ± 5 keV. Figure 1 presents the best-fit spectral parameters and 3–20 keV flux as a function of time, with a time resolution of one observation. The light curve exhibits variability on a timescale of weeks. The peak was reached about 90 days after discovery and is 9 times the lowest flux levels observed thus far. Outside this main peak, the flux occasionally reaches one-half the peak value. There is no obvious periodicity.

We also studied the light curve as measured with the All-Sky Monitor on *RXTE* since 1996. This light curve is quite noisy because of the small flux. There is no conclusive evidence for outbursts other than the one reported here, and there is no indication that XTE J1543–568 was ever brighter than the flux levels measured with the PCA.

2.2. Pulse Period and Binary Orbit

For the study of the pulse period, we employed event data with 0.5 s time resolution and 64 readout channels for photon energy (i.e., configuration E_500us_64M_0_1s). We optimized the accuracy of the pulse period determination as a function of

¹ Also at Space Research Organization Netherlands.

² Also at Universities Space Research Association.

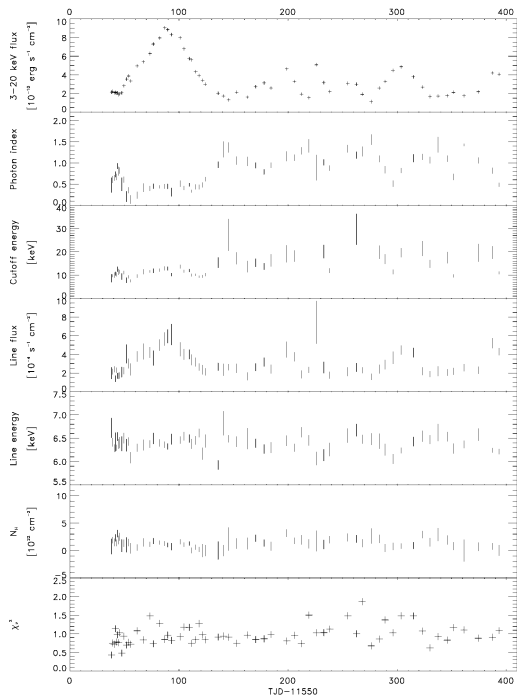


FIG. 1.—*Top panel:* PCA-measured time history of XTE J1543–568 flux in 3–20 keV, from the time of discovery through the first year of monitoring observation. The flux was corrected for small contributions from the transient XTE J1550–564, which was active between TJD 11,640 and 11,690 (Corbel et al. 2001) and resides at the border of the field of view at 1°07 from XTE J1543–568. The errors (not indicated) are typically a few percent. *Second through sixth panels:* Evolution of power-law photon index, e -folding cutoff energy, photon flux and centroid energy of the emission line, and hydrogen column density. For some spectra, the cutoff energy could not be constrained and no data point is given in the appropriate panel. The average hydrogen column density is $(1.3 \pm 0.1) \times 10^{22} \text{ cm}^2$. The emission-line flux follows the overall flux. In fact, the equivalent width is consistent with being constant with a value of 127 eV. *Bottom panel:* χ^2 statistic for the relevant spectral fits.

detector layers and bandpasses and find the best result if all layers are included and photons with energies higher than 20 keV excluded, although this optimum is only marginally better than if only layer 1 is included. We combined the data from all active PCUs, applied standard filters to eliminate bad data, and corrected the resulting light curves to the solar system barycenter. The latter includes a correction for the satellite orbit. For each of the observations, we measured the pulse period by epoch folding the data for a relevant range of test periods and calculating the χ^2 -values for a constant flux hypothesis. The resulting curves show sinc-like trends. To obtain the best-fit period, we fitted for each observation the peak curve with a third-degree polynomial and identified the period with the peak position of the cubic function. The 68% confidence error was estimated by determining the range of periods for which the χ^2 -value is within 1 from the maximum. This procedure was verified through Monte Carlo simulations. The resulting measurements are presented in Figure 2. They are supplemented with 78 BATSE measurements from the public domain³ and from Finger & Wilson (2000), pertaining to TJD 11,572–11,678 (TJD = JD – 2,440,000.5). The BATSE observations stopped prior to deorbiting the satellite in 2000 June. Figure 2 clearly shows that there is a 75 day

³ Made available through the World Wide Web at <http://www.batse.msfc.nasa.gov/batse>.

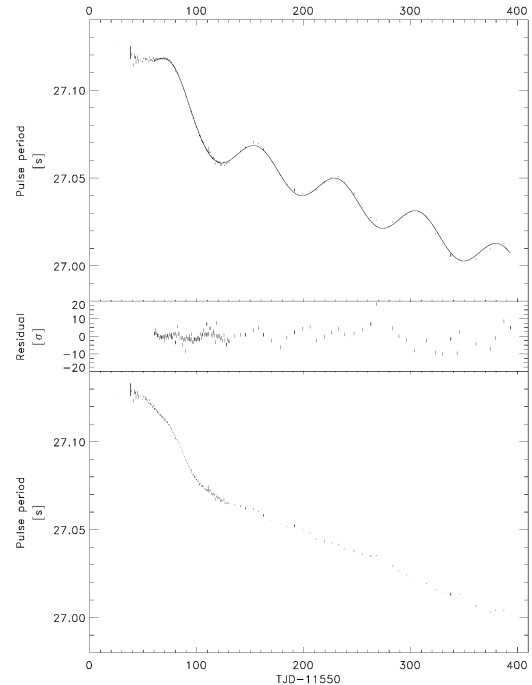


FIG. 2.—Time history of pulse period as measured with the PCA and BATSE. The solid curve shows the fitted model (see text) that was applied to data after TJD 11,610. *Middle:* Residuals of the data points with respect to the fitted model in terms of σ . *Bottom:* Pulse period history after subtraction of the sinusoidal variation. All error bars are without multiplication by 3.2 (see text).

periodicity, which must be due to an expected binary orbit. In addition, long-timescale spin-up trends are visible, which are expected to result from accretion torque. The spin-up is faster in the first ~ 100 days, which is consistent with an accretion torque explanation because the flux and, therefore, the accretion rate is larger at that time.

In order to disentangle the orbital modulation from the spin-up trend, we modeled in an initial step the orbital modulation through a simple sinusoidal variation. The spin-up was modeled through various simple functions with similar success, and we here present the results when the period derivative \dot{P} is described by a Gaussian function on top of a flat, nonzero level. We modeled only the data after TJD 11,610 because the spin-up seems to be more complex before that. For the determination of the orbit this is not detrimental because the excluded time interval represents only about 5% of the complete time span of the observations. The results of the modeling are presented in Figure 2. In a second step, we subtracted the model for the spin-up from the data and fitted a model of an eccentric binary orbit to the residuals. The best-fit χ^2_ν is rather high at 10.2 (for 118 degrees of freedom ν), which we attribute to an incomplete spin-up model. In order to obtain estimates for the errors in the model parameters that take into account the systematic uncertainties, we forced χ^2_ν to 1 through a multiplication of all pulse period errors by a constant factor $\sqrt{10.2} = 3.2$. The results for the orbital and spin-up parameters are given in Table 1. In the bottom panel of Figure 2 we plot the data after subtraction of the orbital modulation model and in Figure 3 after subtraction of the spin-up model and folding with the orbital period. As a double check, we carried out the same procedure for the data after TJD 11,670, which excludes the times when the Gaussian component of the spin-up model is important. Thus, possible

TABLE 1
FIT PARAMETERS TO PULSE PERIOD HISTORY

Fit Parameter	Observed Value	Check Value
Orbital period P_{orb} (days)	75.56 ± 0.25	75.88 ± 0.40
Orbital amplitude (ms)	9.18 ± 0.21	9.07 ± 0.26
Semimajor axis $a_x \sin i$ (lt-s)	353 ± 8	349 ± 20
Eccentricity e	<0.03 at 2σ	<0.03 at 2σ
Epoch of mean longitude $\pi/2$ (TJD)	11725.88 ± 0.16	11725.54 ± 0.62
Pulse period P at TJD 11,600 (s)	27.12156 ± 0.00059	27.1225 ± 0.0043
Constant \dot{P} term (s s^{-1})	$-(2.84 \pm 0.02) \times 10^{-9}$	$-(2.84 \pm 0.03) \times 10^{-9}$
Gaussian \dot{P} term:		
σ (days)	13.30 ± 0.02	
Peak time (TJD)	$11,636.71 \pm 0.02$	
Peak \dot{P} -value (s s^{-1})	$-(1.27 \pm 0.03) \times 10^{-8}$	

NOTE.—The errors are for 68% confidence. The numbers in the third column are, as a reference, from data after TJD 11,670 (40 data points).

strong systematic errors are avoided at the expense of accuracy. The result, given in an extra column in Table 1, is consistent with the previous result.

The pulse profile was studied for three observations throughout the total observation span (see Fig. 4 for the profile at flux peak). The profile consists of two broad peaks at a phase difference of 0.5 and with different magnitudes. The pulsed fraction is consistently $65\% \pm 5\%$. This kind of profile and amplitude is not unusual for pulsars among high-mass X-ray binaries (cf. Bildsten et al. 1997 and White, Nagase, & Parmar 1995). We determined the profiles in two energy bands (2–10 and 10–20 keV) and do not find strong morphological differences. The pulse fraction is about 10% higher in the upper energy band.

3. DISCUSSION

Given the projected semimajor axis $a_x \sin i$ and P_{orb} , we can place constraints on the companion of the neutron star. The mass function is

$$f(M) = \frac{4\pi^2(a_x \sin i)^3}{GP_{\text{orb}}^2} = \frac{(M_c \sin i)^3}{(M_x + M_c)^2} = 8.2 \pm 0.5 M_{\odot}. \quad (1)$$

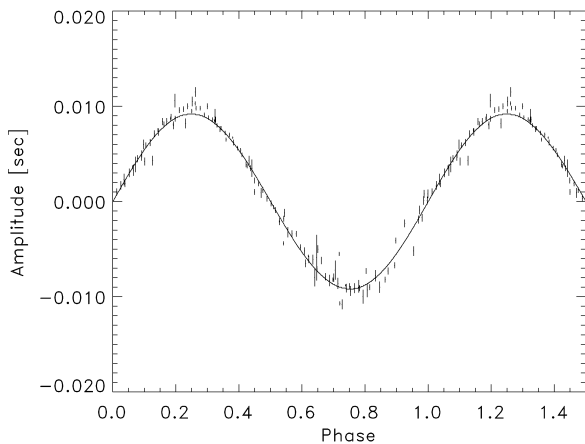


FIG. 3.—Pulse period history for data taken after TJD 11,610, after subtraction of spin-up model and folding with period of 75.56 days. The solid curve shows the solution for the binary orbit, with $e = 0.005$. All error bars are without multiplication by 3.2 (see text).

If $M_x = 1.4 M_{\odot}$, this implies a minimum mass for the companion star of $10.0 M_{\odot}$. For a main-sequence star, the implied spectral type is B3 or earlier (Zombeck 1990). The orbital period places XTE J1543–568 in the “Corbet” diagram of pulse period versus orbital period unambiguously on the branch of optically confirmed Be transients (Corbet et al. 1986; cf. Bildsten et al. 1997).

In principle the distance is constrained by the spin-up rate and flux. The flux is a measure of the mass accretion rate, which determines the torque on the neutron star and the spin-up rate. Given the steadiness of the spin-up rate, we consider it likely that the accretion occurs through a disk. In that case Ghosh & Lamb (1979) predict a spin-up rate of

$$-\dot{P} = 1.9 \times 10^{-12} \mu_{30}^{2/7} m^{-3/7} R_6^{6/7} I_{45}^{-1} P^2 L_{37}^{6/7} \text{ s s}^{-1} \quad (2)$$

for a neutron star with magnetic dipole moment μ_{30} in units of 10^{30} G cm^3 , mass m in units of $1.4 M_{\odot}$, radius R_6 in units of 10 km, moment of inertia I_{45} in units of 10^{45} g cm^2 , and luminosity L_{37} in units of $10^{37} \text{ ergs s}^{-1}$. In Figure 5 we present the period derivative as a function of 3–20 keV flux. Our data are rather noisy and do not cover a large dynamic range in

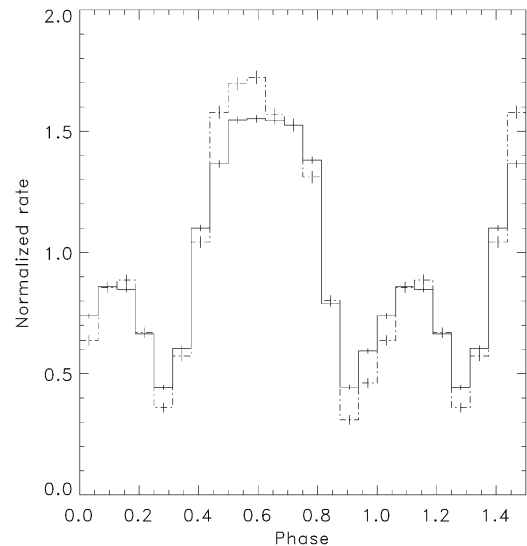


FIG. 4.—Pulse profiles for the observation taken on TJD 11,637, when the peak flux was reached. The solid histogram is for 3–10 keV, the dashed one for 10–20 keV.

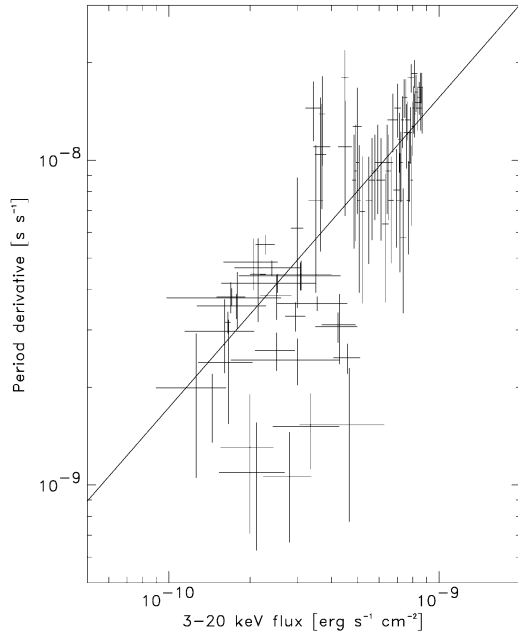


FIG. 5.—Period derivative, as determined from BATSE and *RXTE* data points, vs. 3–20 keV flux. The baseline for each period derivative determination was three observations (or at least 2 days). The error bars on the flux represent the range of fluxes measured during this baseline. The solid line is the best-fit power-law function, with index 0.95 ± 0.06 .

flux, but they appear to be roughly consistent with a $\frac{6}{7}$ power-law relationship. Given the spectral shapes found, the overall bolometric correction is about a factor of 2. If we calibrate the above $-\dot{P}/L_{37}$ relation at the $-\dot{P} = 1 \times 10^{-8} \text{ s s}^{-1}$ level and assume all normalized parameters to be 1, the implied distance is 26 kpc. This would place XTE J1543–568 at an unlikely position. Acceptable distances would perhaps be at least about 50% smaller. It is hard to achieve that by adjusting the other parameters individually: μ_{30} would have to be at least 64 times larger, m 16 times smaller, R_6 4 times larger, or I_{45} 3 times smaller. Therefore, given the correctness of the Ghosh & Lamb formulation, there is at least the suggestion that the distance is large.

Another constraint for the distance, which does not require μ , may be obtained from an argument over the magnetospheric radius r_{mag} at which the neutron star magnetosphere begins to dictate the mass flow. This radius scales with $\dot{M}^{-2/7}$ or $F^{2/7}$. If the flux F varies between F_{min} and F_{max} at times when the mass accretion persists, $r_{\text{mag}} < r_{\text{co}}(F_{\text{min}}/F_{\text{max}})^{2/7}$ at peak flux, where r_{co} is the corotation radius at which the Keplerian period is equal to the spin period [$r_{\text{co}} = (GMP^2/4\pi^2)^{1/3}$]. The torque $2\pi I\dot{\nu}$ is given by $\dot{M}(GMr_{\text{mag}})^{1/2}$. Substitution in the above con-

dition reveals

$$\dot{M} > -5.6 \times 10^2 \frac{I_{45}\dot{P}}{m^{2/3}P^{7/3}(F_{\text{min}}/F_{\text{max}})^{1/7}} M_{\odot} \text{ yr}^{-1}. \quad (3)$$

For standard parameters and $F_{\text{max}} = 4.5F_{\text{min}}$ (after TJD 11,670), we obtain $\dot{M} > 9.8 \times 10^{-10} M_{\odot} \text{ yr}^{-1}$. If all liberated potential energy is released in the form of radiation, the bolometric luminosity is constrained by $L > 1.2 \times 10^{37} \text{ ergs s}^{-1}$. For $F_{\text{max}} = 4.5 \times 10^{-10} \text{ ergs s}^{-1} \text{ cm}^{-2}$ and a bolometric correction of 2, a minimum distance of 10 kpc is implied. Again, this is a fairly large distance.

These distance estimates suggest that searches for the optical counterpart may prove difficult, also because the large value of N_{H} points to a high extinction. For a $10.0 M_{\odot}$ main-sequence star, $M_V = -2$. If $N_{\text{H}} = 1.3 \times 10^{22}$ (see Fig. 1; this is consistent with the total Galactic column as inferred from maps by Dickey & Lockman 1990), $A_V = 7.4$ (according to the standard conversions introduced by Predehl & Schmitt 1995). For a distance of 26 kpc, the apparent visual magnitude would be $V = 23$, and, for a distance of 10 kpc, $V = 21$.

The most interesting result of our analysis is the low eccentricity. It is among the lowest for the 12 confirmed or suspected Be X-ray binaries whose orbits have now been determined (eight cases are reviewed by Bildsten et al. 1997, and since then orbits have been determined for 2S 1845–024 by Finger et al. 1999, for SAX J2103.5+4545 by Baykal, Stark, & Swank 2000, and for X Per by Delgado-Martí et al. 2001). There is one other system apart from XTE J1543–568 that has an eccentricity that is consistent with 0 ($e < 0.09$ at 2σ confidence for 2S 1553–54; see Kelley, Rappaport, & Ayasli 1983). However, one should note that Kelley et al. have a sparse coverage of less than one binary orbit and do not solve for spin-up. Finding low-eccentricity systems is remarkable because one would expect most long-period Be systems to have undergone supernovae with large kick velocities for the neutron stars and to have circularization timescales far longer than their ages. XTE J1543–568 confirms the suspicion that there may be a substantial population of neutron stars formed with little or no kick (Delgado-Martí et al. 2001).

We thank the project scientist Jean Swank for continuing the *RXTE* observations of XTE J1543–568 through public TOOs after our TOO program time was spent, Evan Smith for his tireless efforts to schedule the many observations, Mike Tripicco for his assistance in the barycentric corrections for 2001 PCA data, Ron Remillard for his advice on the ASM light curve, and the referee Mark Finger for valuable suggestions. J. M. i. Z. acknowledges financial support from the Netherlands Organization for Scientific Research.

REFERENCES

- Baykal, A., Stark, M., & Swank, J. 2000, *ApJ*, 544, L129
 Bildsten, L., et al. 1997, *ApJS*, 113, 367
 Corbel, S., et al. 2001, *ApJ*, 554, 43
 Corbet, R. H. D. 1986, *MNRAS*, 220, 1047
 Delgado-Martí, H., Levine, A. M., Pfahl, E., & Rappaport, S. A. 2001, *ApJ*, 546, 455
 Dickey, J. M., & Lockman, F. J. 1990, *ARA&A*, 28, 215
 Finger, M. H., Bildsten, L., Chakrabarty, D., Prince, T. A., Scott, D. M., Wilson, C. A., Wilson, R. B., & Zhang, S. N. 1999, *ApJ*, 517, 449
 Finger, M. H., & Wilson, C. A. 2000, *IAU Circ.*, 7366
 Ghosh, P., & Lamb, F. K. 1979, *ApJ*, 234, 296
 Jahoda, K., Swank, J. H., Stark, M. J., Strohmayer, T., Zhang, W., & Morgan, E. H. 1996, *Proc. SPIE*, 2808, 59
 Kaptein, R. G., in 't Zand, J. J. M., & Heise, J. 2001, *IAU Circ.*, 7588
 Kelley, R. L., Rappaport, S., & Ayasli, S. 1983, *ApJ*, 274, 765
 Marshall, F. E., Takeshima, T., & in 't Zand, J. J. M. 2000, *IAU Circ.*, 7363
 Morrison, R., & McCammon, D. 1983, *ApJ*, 270, 119
 Predehl, P., & Schmitt, J. H. M. M. 1995, *A&A*, 293, 889
 White, N. E., Nagase, F., & Parmar, A. N. 1995, in *X-Ray Binaries*, ed. W. H. G. Lewin, J. van Paradijs, & E. P. J. van den Heuvel (Cambridge: Cambridge Univ. Press), 1
 Zombeck, M. V. 1990, *Handbook of Space Astronomy and Astrophysics* (2d ed.; Cambridge: Cambridge Univ. Press)